

Les Premières Données dans ATLAS et le Calorimètre à Argon Liquide Des muons cosmiques aux premières collisions

S. Laplace, P. Iengo
Pour le groupe ATLAS-LAPP

Plan:

- × Introduction
- × Commissioning du calo Lar (muons+beam splashes)
- × Résultats des premières collisions

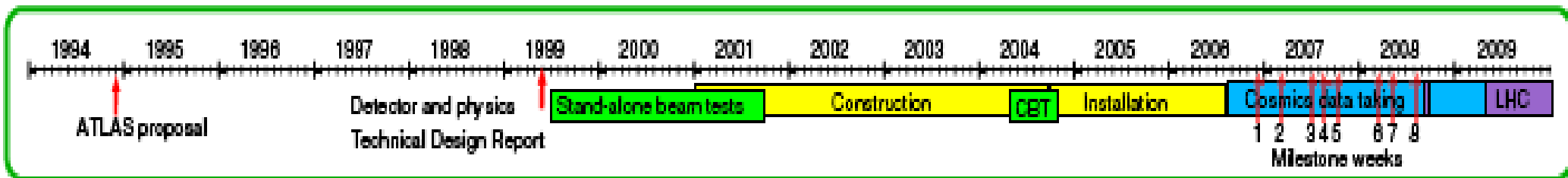
Remarque: le logo



signifie que le LAPP a contribué à l'analyse montrée

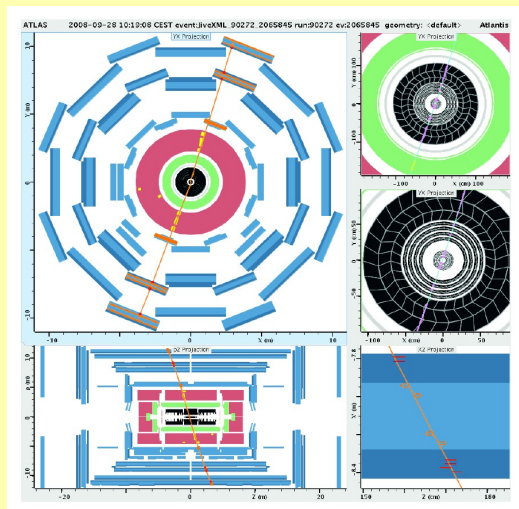
ATLAS In-Situ Commissioning Steps

- In situ commissioning of ATLAS detectors ongoing since 4 years:



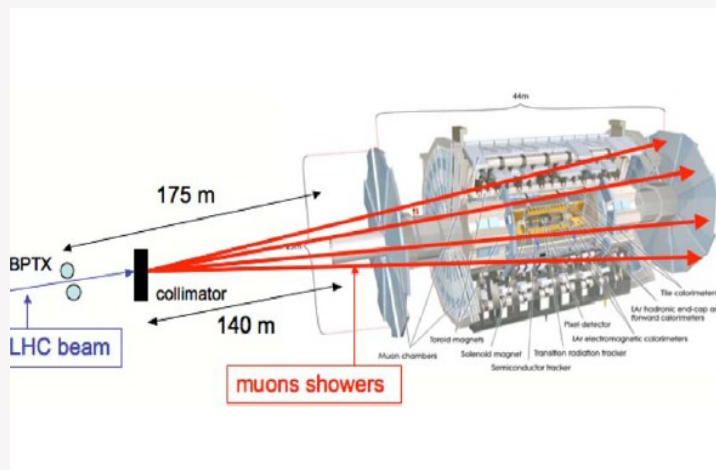
Cosmic muons (since 2006)

Muon: Minimum Ionizing Particle (MIP) in LAr calorimeter



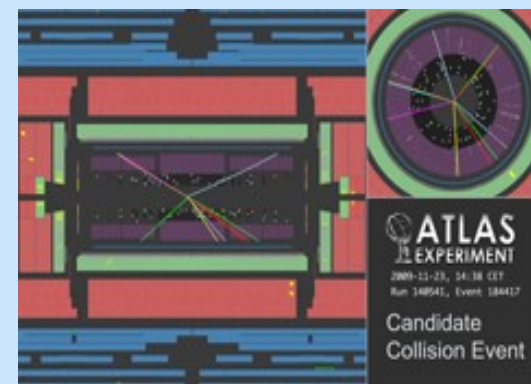
First LHC Beams (Sept. 10-12, 2008)

Very large energy deposited in most of LAr cells !



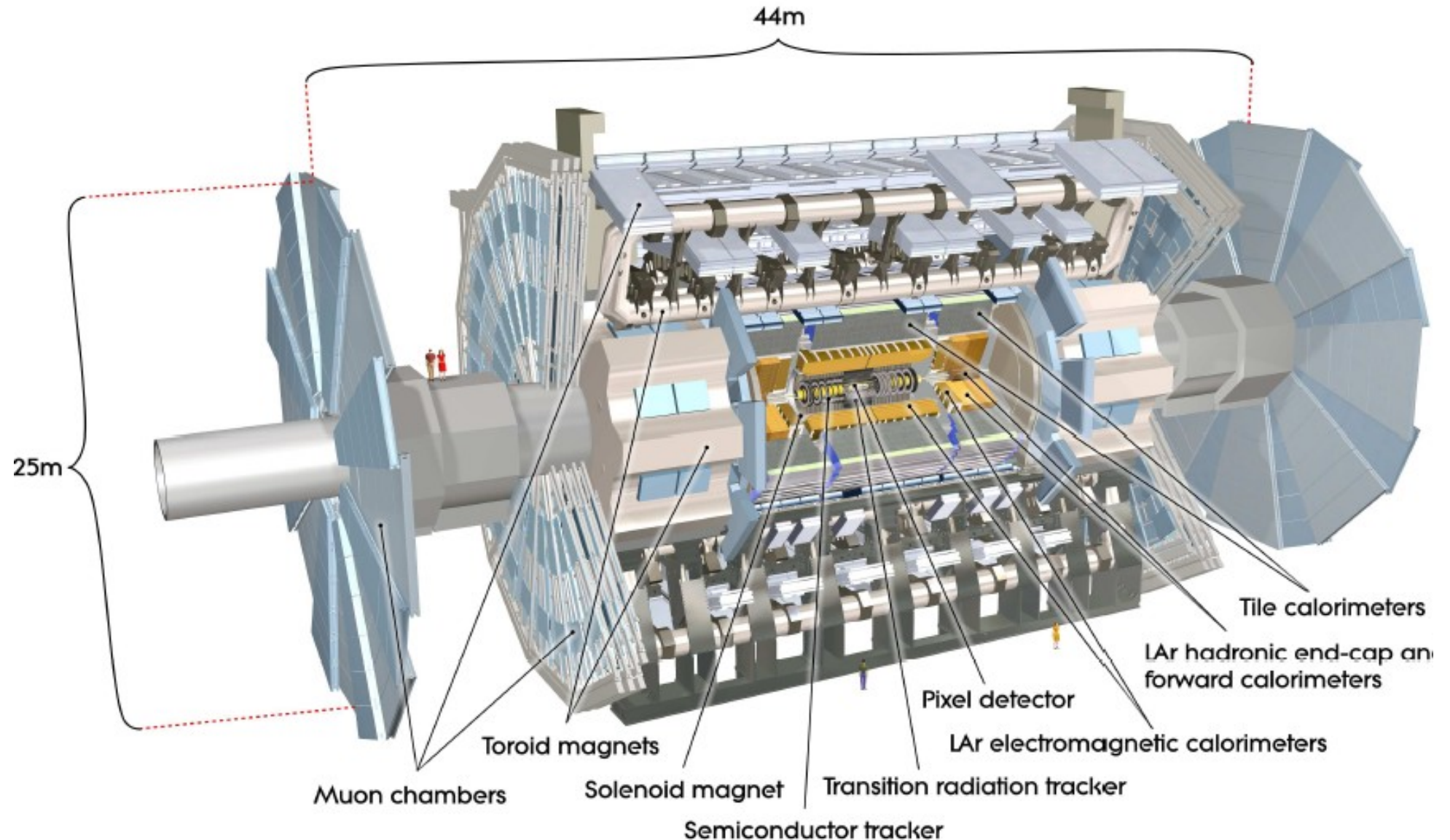
First Collisions (Nov. 23, 2009)

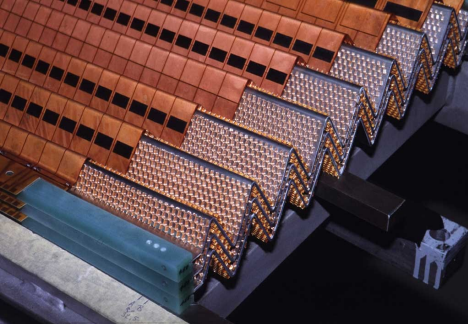
Real events !



Detector component	Required resolution	η coverage	
		Measurement	Trigger
Tracking	$\sigma_{p_T}/p_T = 0.05\% \ p_T \oplus 1\%$	± 2.5	
EM calorimetry	$\sigma_E/E = 10\%/\sqrt{E} \oplus 0.7\%$	± 3.2	± 2.5
Hadronic calorimetry (jets) barrel and end-cap forward	$\sigma_E/E = 50\%/\sqrt{E} \oplus 3\%$	± 3.2	± 3.2
	$\sigma_E/E = 100\%/\sqrt{E} \oplus 10\%$	$3.1 < \eta < 4.9$	$3.1 < \eta < 4.9$
Muon spectrometer	$\sigma_{p_T}/p_T = 10\%$ at $p_T = 1$ TeV	± 2.7	± 2.4

ATLAS

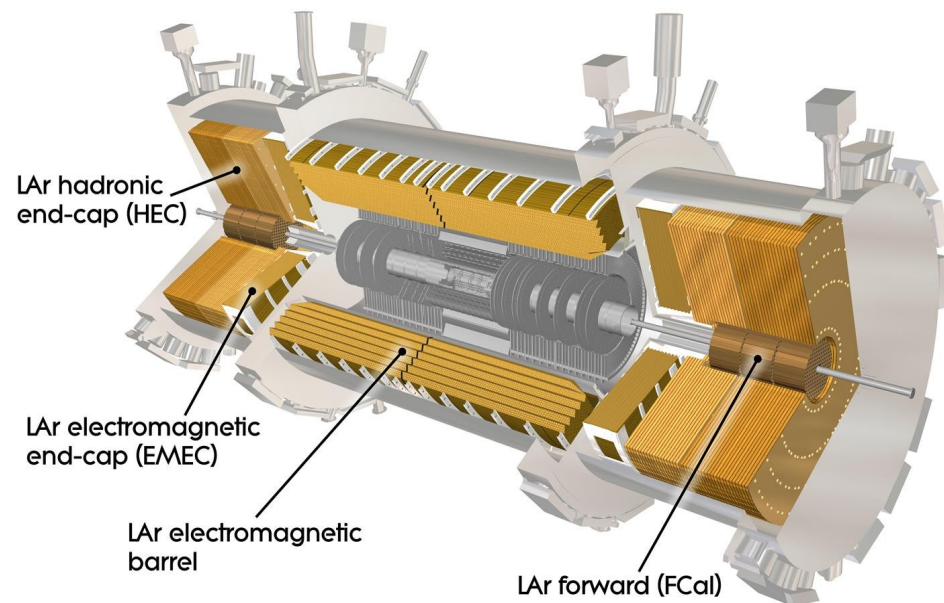




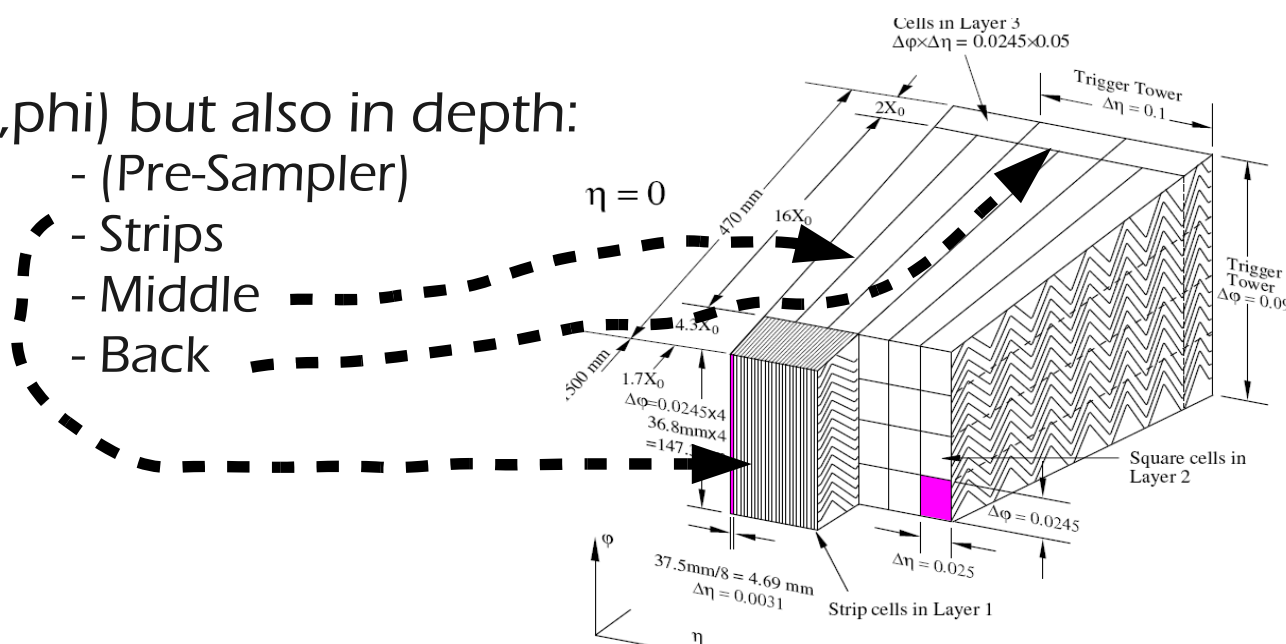
Introduction to the ATLAS

LAr Calorimeter (1/3)

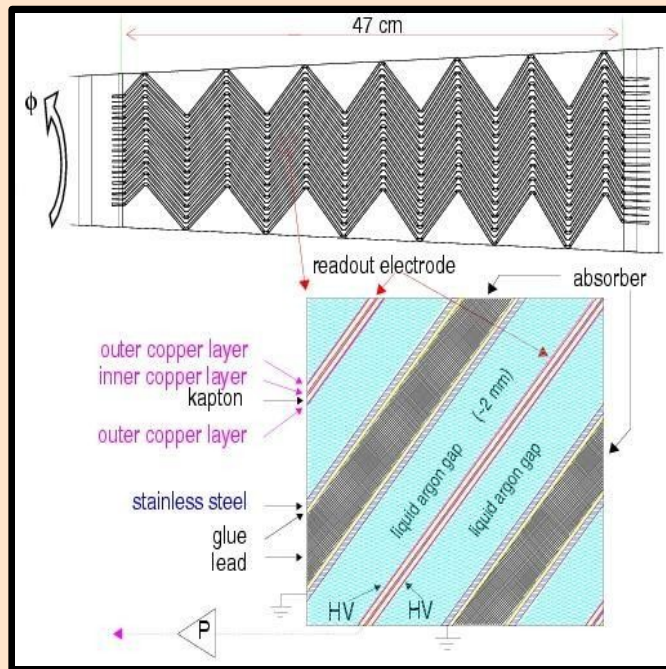
- **Sampling calorimeters:** LAr+Pb/Cu/W
- **Standard barrel/endcap structure:**
 - barrel ($|\eta| < 1.4$): electromagnetic (EM)
 - endcap ($|\eta| < 4.9$): EM+ hadronic (HAD) + forward (FCAL)
 - presampler up to $|\eta| = 1.8$



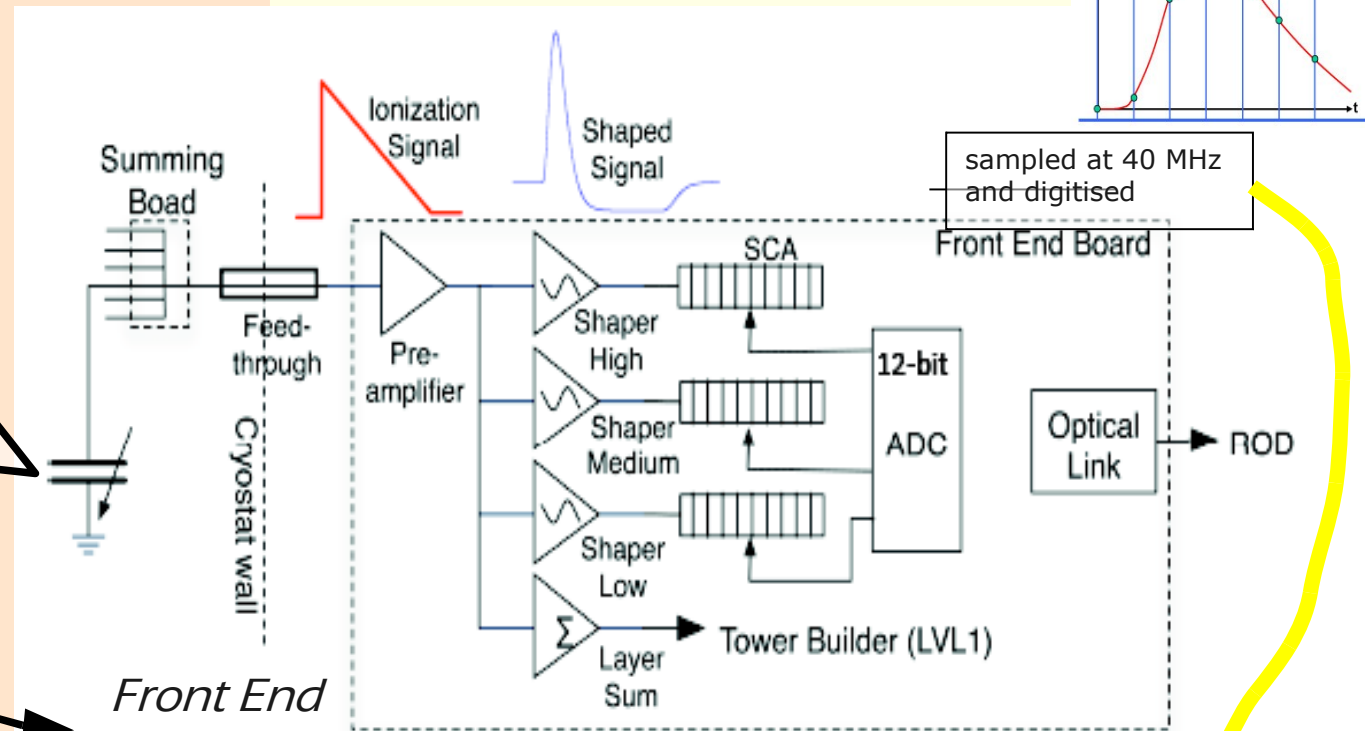
- **Segmentation:** lateral (eta, phi) but also in depth:
 - (Pre-Sampler)
 - Strips
 - Middle
 - Back
- **Energy resolution:**
 - $\sigma/E \sim 10\%/\sqrt{E} \oplus 0.7\%$ (EM)
 - $\sigma/E \sim 50\%/\sqrt{E} \oplus 3\%$ (HAD)
 - $\sigma/E \sim 100\%/\sqrt{E} \oplus 10\%$ (FCAL)



Introduction to the ATLAS LAr Calorimeter (2/3)



Calorimeter



Front End Electronics

Back End Electronics

Phys/Cal Difference

ADC to DAC (Ramps)

Pulse Samples

$$E_{\text{cell}} = F_{\mu\text{A} \rightarrow \text{MeV}} \cdot F_{\text{DAC} \rightarrow \mu\text{A}} \cdot \frac{1}{M_{\text{phys}} / M_{\text{cali}}} \cdot R \left[\sum_{j=1}^{N_{\text{samples}}} a_j (s_j - p) \right]$$

Energy

Energy Conversion

Calibration board

Optimal Filtering Coefficients

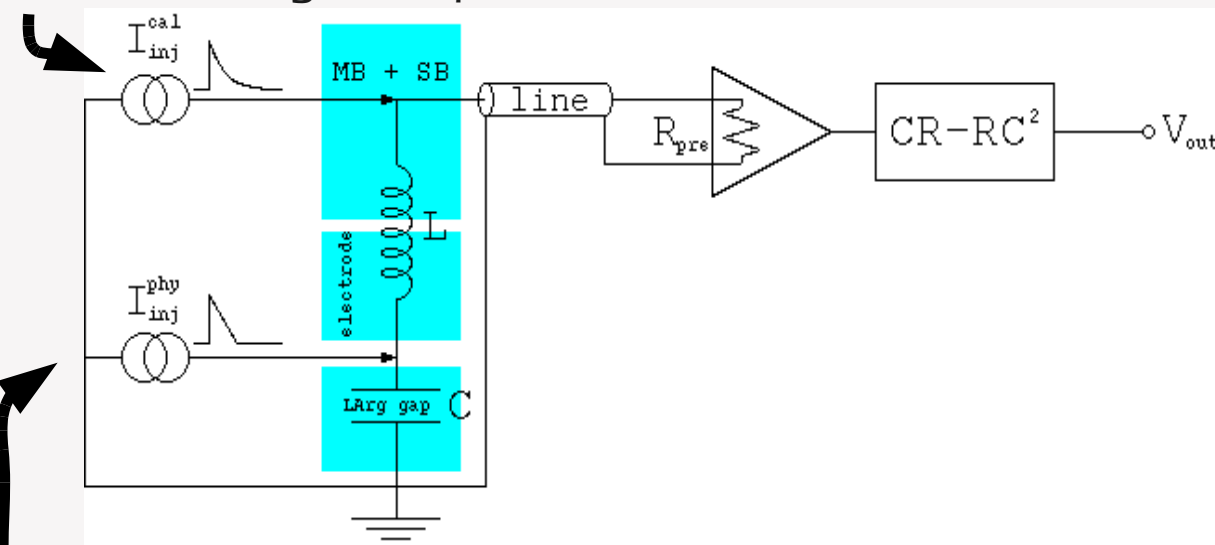
Pedestals

Introduction to the ATLAS

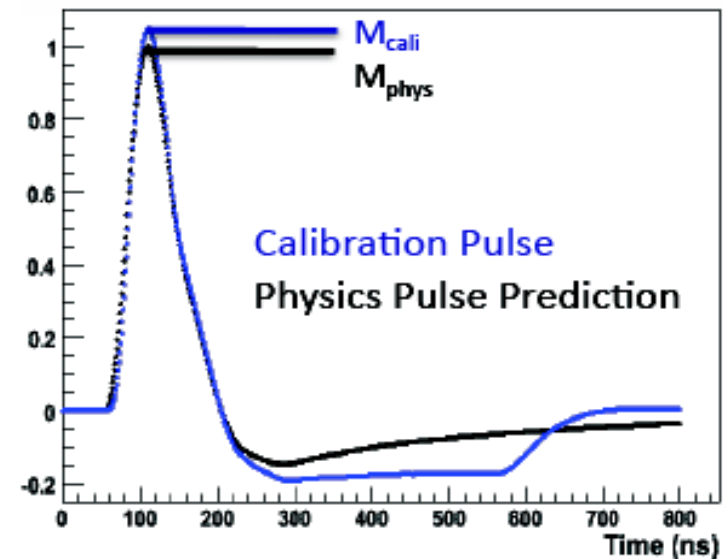
LAr Calorimeter (3/3): The Calibration System

- Used to compute several electronics-related constants, including optimal filtering coefficients
- Calibration and physics pulse are different due to different injected signal and injection points: methods exist to predict physics pulses from calibration pulse

Calibration signal: exponential



Physics signal: triangular

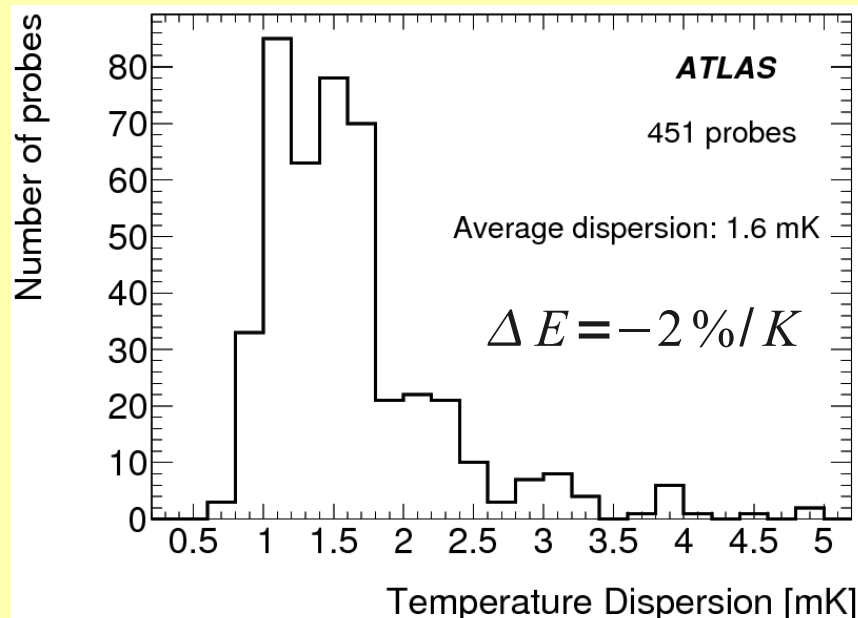


ATLAS Status

Subdetector	Number of Channels	Approximate Operational Fraction
Pixels	80 M	97.9%
SCT Silicon Strips	6.3 M	99.3%
TRT Transition Radiation Tracker	350 k	98.2%
LAr EM Calorimeter	170 k	98.8%
Tile calorimeter	9800	99.2%
Hadronic endcap LAr calorimeter	5600	99.9%
Forward LAr calorimeter	3500	100%
MDT Muon Drift Tubes	350 k	99.7%
CSC Cathode Strip Chambers	31 k	98.4%
RPC Barrel Muon Trigger	370 k	98.5%
TGC Endcap Muon Trigger	320 k	99.4%
LVL1 Calo trigger	7160	99.8%

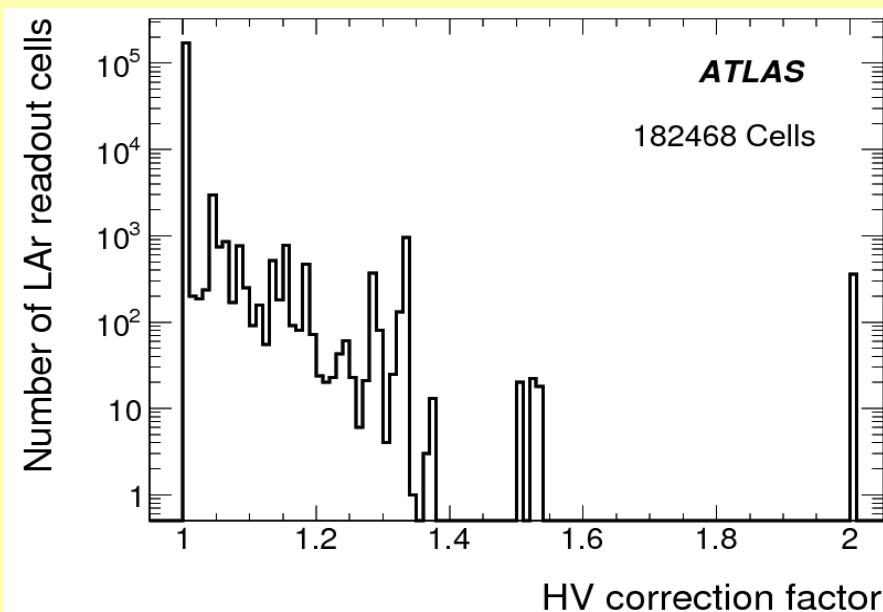
Calorimeter Status

LAr temperature



Typical cryostat uniformity: 70-80 mK
[requirement < 100 mK \rightarrow $c < 0.2\%$]

High-Voltage



Nominal HV cells: 93.9%
No dead HV region (corrections)

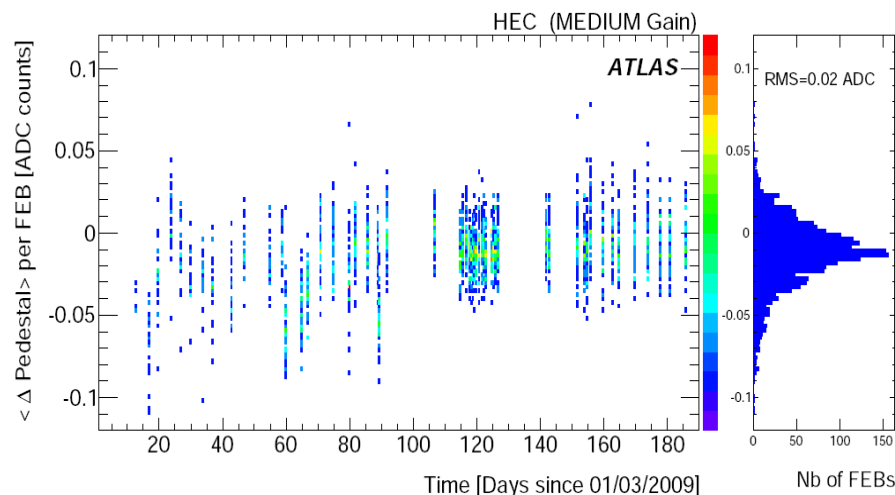
LAr Readout status (as of end of Sept. 2009):

- 98.7% cells used in reconstruction
- 1.3% remaining:
 - 1.2% (19) inactive FEBs (dead OTx)
 - 0.1% of problematic cells:
 - 0.02% dead
 - 0.03% permanently noisy
 - 0.07% sporadically noisy

Can recover energy for jet/ETmiss
using trigger tower energy

Calibration Constants Stability

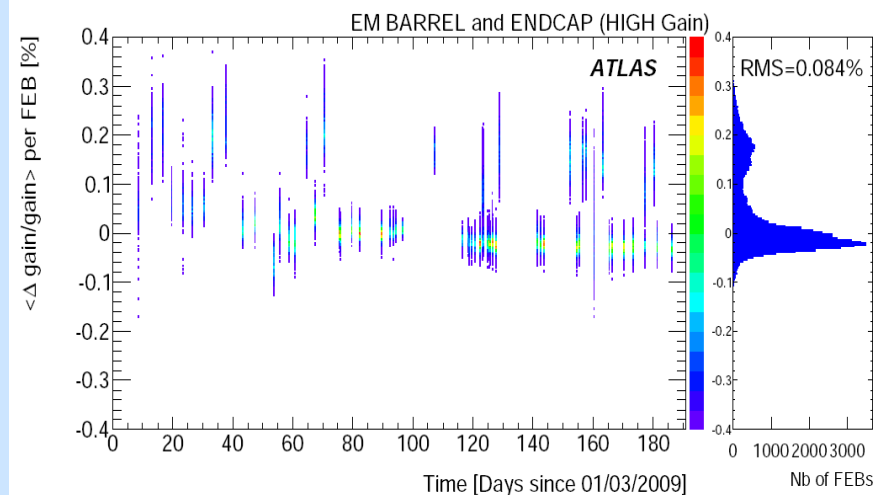
Pedestal



Pedestal variations
 \ll numerical
 precision on E

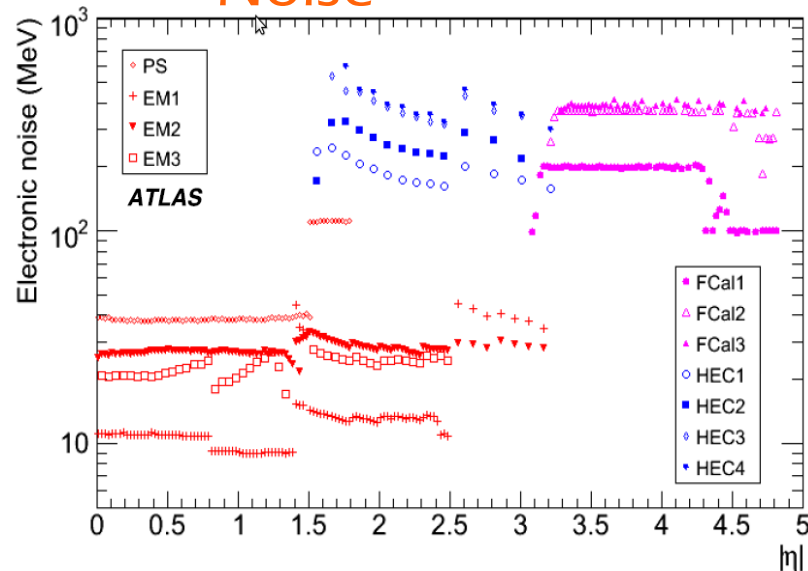


Ramp



Ramp variations $< 0.3\%$
 and corrected after
 each run

Noise



- Noise variations negligible
- Coherent noise = 2%
 (< requirement = 5%)

Calorimeter Readiness for LHC Collisions



Results from random triggers, cosmics muons and first beams:

- Timing Alignment
- dE/dx in calo
- Ionization pulse shapes
- Ion drift time measurement (dedicated paper in prep.)
- Missing Transverse Energy
- Calorimeter Uniformity

All these results are (almost) published in EPJC: **FIRST ATLAS paper !**

EPJ manuscript No.
(will be inserted by the editor)

Readiness of the ATLAS Liquid Argon Calorimeter for LHC Collisions

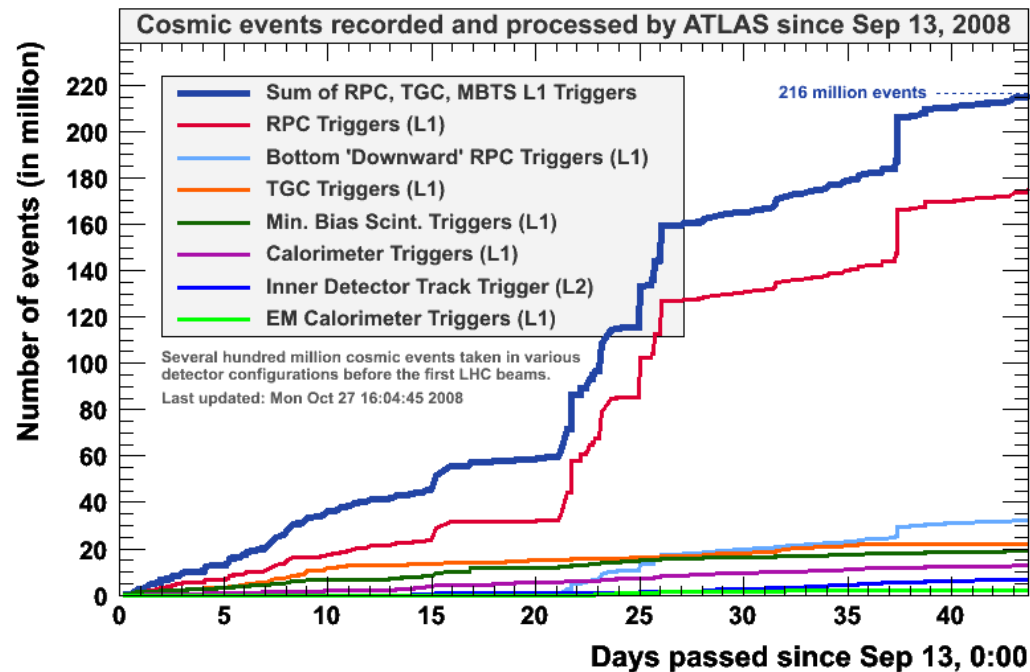
G. Aad⁸³, B. Abbott¹¹⁰, J. Abdallah¹¹, A.A. Abdelalim⁴⁹, A. Abdesselam¹¹⁷, O. Abdinov¹⁰, B. Abi¹¹¹, M. Abolins⁸⁸, H. Abramowicz¹²¹, H. Abreu¹¹⁴, B.S. Acharya^{162a,162b}, D.L. Adams²⁴, T.N. Addy⁵⁶, J. Adelman¹⁷³, C. Adorisio^{36a,36b}, P. Adragna⁷⁵, T. Adye¹²⁸, S. Aefsky²², J.A. Aguilar-Saavedra^{123a}, M. Aharrouche⁸¹, S.P. Ahlen²¹, F. Ahles⁴⁸, A. Ahmad¹⁴⁶, H. Ahmed², M. Ahsan⁴⁰, G. Aielli^{132a,132b}, T. Akgocan¹⁸, T.P.A. Åkesson⁷⁹, G. Akimov¹⁵³, A.V. Akimov⁹⁴, A. Aktas⁴⁸, M.S. Alam¹, M.A. Alam⁷⁸, J. Albert¹⁶⁷, S. Albrand⁵⁵, M. Aleksov²⁹, I.N. Aleksandrov⁶⁸, F. Alessandria^{89a,89b}, C. Alexa^{25a}, G. Alexander¹⁵¹, G. Alexandre⁴⁹, T. Alexopoulos⁹, M. Alhroob²⁰, M. Aliev¹⁵, G. Alimonti^{139a}, J. Alison¹¹⁹, M. Aliyev¹¹⁹, P.P. Allport⁷³, S.E. Allwood-Spiers⁵, J. Almond¹²¹, A. Aloisio^{152a,152b}, R. Alon¹⁴⁹, A. Alonso⁷⁹, M.G. Alviggi^{102a,102b}, K. Amako⁶⁹, C. Amelung²³, V.V. Ammosov¹²⁷, A. Amorim^{123c}, G. Amos¹⁴⁸, N. Anagnostou¹⁷⁴, C. Anastopoulos¹³⁸, T. Andeen²⁹, C.F. Anders⁹⁸, K.J. Anderson³⁰, A. Andreazza^{89a,89b}, V. Andreev^{16a}, X.S. Anduaga⁷⁰, A. Angerami³⁴, F. Anghinolli²⁹, N. Anjos^{123b}, A. Antonak⁸, M. Antonelli⁸⁷, S. Antonelli^{139a,139b}, B. Antunovic⁴¹, P. Anulli^{131a}, S. Aoun⁸³, G. Arabidze⁸, I. Aracena¹⁴², Y. Ara¹⁰, A.T.H. Arce¹⁴, J.P. Archambault²⁸, S. Arfaoui^{29a}, J.-F. Arguin¹⁴, T. Argyropoulos⁸, E. Arkin^{18a}, M. Arkin¹⁸, A.J. Armbruster⁸⁷, O. Arnarez², C. Arnault¹¹⁴, A. Artamonov⁹⁵, D. Arutinov²⁰, M. Asai¹⁴², S. Asai¹⁵³, R. Asfandiyarov¹⁷⁰, S. Ask⁵², B. Åsman¹⁴⁴, D. Asner²⁸, L. Asquith⁷⁷, K. Assamagan²⁴, A. Astbury¹⁶⁷, A. Astvatsatourian⁵², G. Atoian¹⁷³, B. Auerbach¹⁷³, E. Auge¹¹⁴, K. Augsten¹²⁶, M. Aurousseau⁴, N. Austin⁷³, G. Avolio¹⁶¹, R. Avramidou⁹, D. Axen¹⁶⁶, C. Ay⁸⁴, G. Azuelos^{93,9}, Y. Azuma¹⁵³, M.A. Baak²⁹, G. Baccaglioni^{89a,89b}, C. Bacci^{123a,133b}, A. Bach¹⁴, H. Bachacou¹²⁸, K. Bachas²⁹, M. Backes⁴⁹, E. Badescu^{29a}, P. Bagnaia^{131a,131b}, Y. Bai³², D.C. Bailey¹⁶⁶, T. Bain¹⁶⁶, J.T. Baines¹²⁸, O.K. Baker¹⁷³, M.D. Baker²⁴, F. Baltasar Dos Santos Pedros²⁹, E. Banas¹⁸, P. Banerjee²⁰, S. Banerjee¹⁶⁷, D. Banfi^{89a,89b}, A. Bangert¹³⁶, V. Bansal¹⁶⁷, S.P. Baranov²⁴, S. Baranov⁸, A. Barashkou⁶⁵, T. Barber²⁷, E.L. Barberio⁶⁶, D. Barberis^{89a,89b}, M. Barbero²⁹, D.Y. Bardin⁶⁵, T. Barillari²⁹, M. Barisonzi¹⁷², T. Barkow¹⁴², N. Barlow⁷, B.M. Barnett¹²⁸, R.M. Barnett¹⁴, S. Baron²⁹, A. Barone^{133a}, A.J. Barr¹⁷, F. Barreiro⁸⁰, J. Barreiro Guimarães da Costa²⁷, P. Barrillon¹⁴, N. Barnes^{123b}, R. Bartoldus¹⁴², D. Bartosch²⁰, J. Bastos^{123b}, R.L. Bates⁸³, S. Bathe²⁴, L. Batkova¹⁴¹, J.R. Batley²⁷, A. Battaglia¹⁶, M. Battistini²⁹, F. Bauer¹³⁸, H.S. Bawa¹⁴², M. Bazalova¹²⁴, B. Beare¹⁶⁶, T. Beau⁷⁸, P.H. Beauchemin¹¹⁷, R. Beccherini⁸, N. Becherini¹⁸, P. Bechtel⁴¹, G.A. Beck⁷⁹, H.P. Beck¹⁸, M. Beckingham⁴⁸, K.H. Beckers¹⁷², I. Bedjane¹²⁶, A.J. Beddall^{18a}, A. Beddall^{18a}, P. Bednarek¹⁴³, V.A. Bednyakov⁶⁵, C. Bee⁸³, M. Begg²⁴, S. Behar Harpaz¹⁵⁰, P.K. Behara⁶³, M. Belforte²⁹, C. Belanger-Champagne¹⁶⁴, P.J. Bell⁸², W.H. Bell⁴⁹, G. Bella¹⁸¹, L. Bellagamba^{19a}, F. Bellina²⁹, M. Bellomo^{118a}, A. Belloni⁸⁷, K. Belotskiy⁹⁶, O. Beltramello²⁹, S. Ben Ami¹⁹⁰, O. Benary¹⁸¹, D. Benchebrouk^{134a}, M. Bendat⁸¹, B.H. Benedict¹⁶¹, N. Benekos¹⁶³, Y. Benhammou¹⁸¹, G.P. Benincasa^{123b}, D.P. Benjamin¹⁴, M. Benoit¹¹⁴, J.R. Bensinger²², K. Benslama¹²⁹, S. Bentvelsen¹⁰⁸, M. Beretta⁴⁷, D. Berge²⁹, E. Bergeas Kuitmann¹⁴⁴, N. Berger⁴, F. Berghaus¹⁶⁷, E. Berglund⁴⁹, J. Beringer¹⁴, K. Bernabetti⁸³, P. Bernat¹¹⁴, R. Bernhart⁴⁸, C. Bernius⁷, T. Berry⁷⁸, A. Bertin^{19a,19b}, N. Besson¹³⁵, S. Bethke²⁹, R.M. Bianchi⁴⁸, M. Bianco^{72a,72b}, O. Biebel²⁶, J. Biesiad¹⁴, M. Biglietti^{131a,131b}, H. Bilokon⁴⁷, M. Bindi^{129a,19b}, S. Binet¹¹⁴, A. Bingul^{15a}, C. Bini^{131a,131b}, C. Biscarat¹⁷⁸, U. Bitenc⁴⁸, K.M. Black²⁷, R.E. Blair¹, J.-B. Blanchard¹¹⁴, G. Blanchot²⁹, C. Blocker²², J. Blocki¹, A. Blondel⁴⁹, W. Blum¹, U. Blumenschein¹, G.J. Bobbink^{19a}, A. Bocci¹⁴⁴, M. Boehler¹, J. Boek¹⁷², N. Boelaert⁷, S. Böser⁷⁷, J.A. Bogart²⁹, A. Bogouch^{90a}, C. Bolchini¹⁴⁴, J. Böhm¹²⁴, V. Boisvert⁷⁶, T. Boldi¹⁴², V. Boldizsar^{29a}, S. Bolkvadze⁸⁷, V.G. Bondarenko²⁶, M. Bondini¹⁶¹, M. Bonenkamp¹³⁸, J.R.A. Booth¹⁷³, S. Bordoni¹²⁸, C. Borja¹⁶, A. Borisyak¹²⁷, G. Borisyak⁷¹, I. Borjanovic^{78a}, S. Borroni^{131a,131b}, K. Bos¹⁰⁸, D. Boscherini^{19a}, M. Botman¹¹, M. Bostaeus²⁹, H. Boterndorff¹⁰⁵, J. Bouchami⁸³, J. Boudreau¹²², E.V. Bouhoua-Thacker⁷¹, C. Boulhoucha¹²², C. Bourdarios¹¹⁴, J. Boyd²⁹, I.R. Boyko⁶⁸, I. Bozovic-Jelencic¹²⁶, J. Bracinik¹⁷, A. Brancat²⁹, P. Branciani^{133a}, G.W. Brandenburg²⁷, A. Brandt⁷, G. Brandt⁴¹, O. Brandt⁸⁴, U. Bratzler¹⁴⁴, B. Brau⁸⁴, J.E. Brau¹¹³, H.M. Brau¹⁷², B. Bräuer¹⁶⁶, J. Bremer²⁹, R. Brenner¹⁶⁴, S. Bressler¹⁵⁰, D. Breton¹¹⁴, N.D. Brett¹¹⁷, D. Britton⁵⁴, F.M. Brochu²⁷, I. Brock²⁰, R. Brock⁵⁸, T.J. Brodbeck⁷¹, E. Brodeur¹⁸¹, F. Broggi^{89a,89b}, C. Bromberg⁸⁸, G. Broccijmans⁴⁴, W.K. Brooks¹⁵¹, G. Brown⁸², E. Brubaker²⁰, P.A. Bruckman de Renstrom³⁸, D. Bruncko¹⁴³, R. Brunelero⁸, S. Brunet⁴¹, A. Bruni^{19a}, G. Bruni^{19a}, M. Bruschini¹²⁸, T. Buane¹³, F. Buccini⁴⁹, J. Buchanan¹¹⁷, P. Buchholz⁴⁰, A.G. Buckley^{77a}, I.A. Budagov⁹⁸, B. Budick¹⁰⁷, V. Büscher¹, L. Bugge¹¹⁶, O. Bulekov²⁹, M. Bunse⁴², T. Buran¹¹⁶, H. Burkhardt²⁹, S. Burdin⁷³, T. Burgess¹³, S. Burke¹²⁸, E. Busato⁸³, P. Bussey⁸³, C.P. Buszel¹⁶¹, F. Butin²⁹, B. Butler¹⁴², J.M. Butler²¹, C.M. Buttar³¹, J.M. Butterworth⁷⁷, T. Byatt¹⁷, J. Caballero²⁴, S. Cabrera Urbán¹⁰⁸, D. Cafiora^{19a,19b}, O. Cakir⁶, C. Cafarella¹⁴, G. Cakirli¹⁷, P. Calgayan⁸, R. Calkins⁸,

arXiv:0912.2642

Cosmic Data Taking



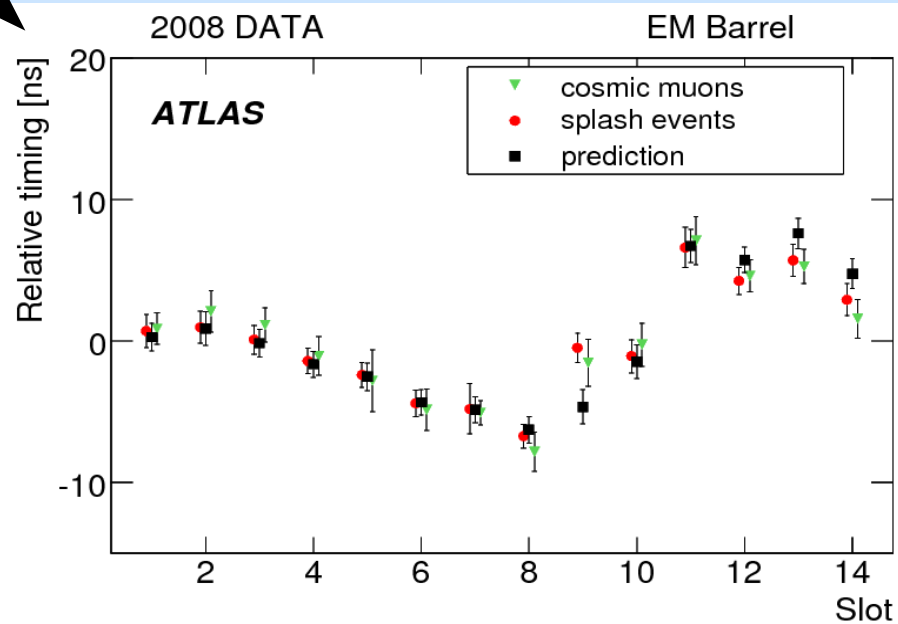
- Long cosmic runs in September-october 2008 and june-july 2009: more than 300 million events were recorded (>500 TB of data)
- Triggers used for studies preented here:
 - L1: muon chambers, L1Calo
 - L2: inner detector tracks



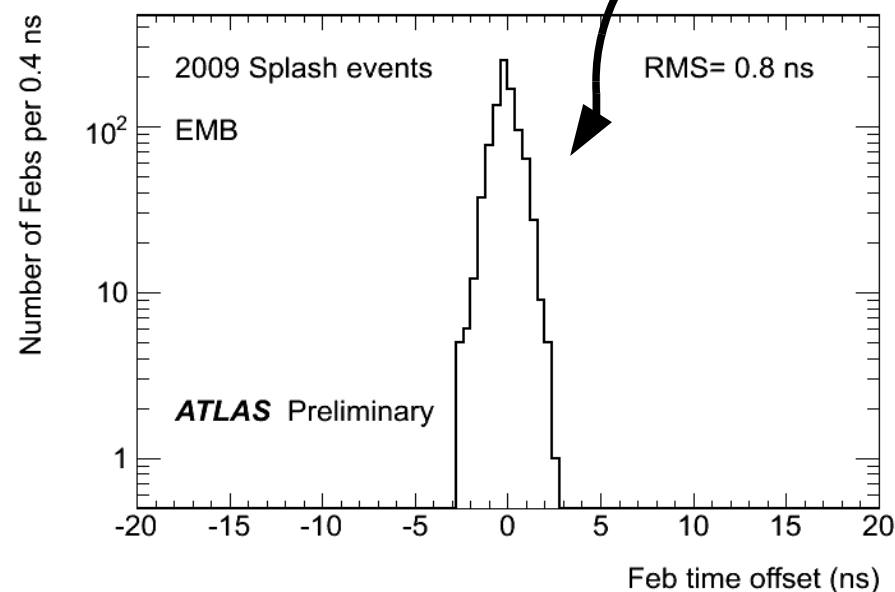
Timing Alignment



- Predicted (=calibration) versus measured (=physics) timing:
 - Measurement: time obtained from Optimal Filtering algorithm + time of flight correction
 - Prediction: calibration pulse + readout path
- Adjustable delay per Front End Board (FEB): obtain values for first collisions



Agreement with prediction
better than $\pm 2\text{ ns}$

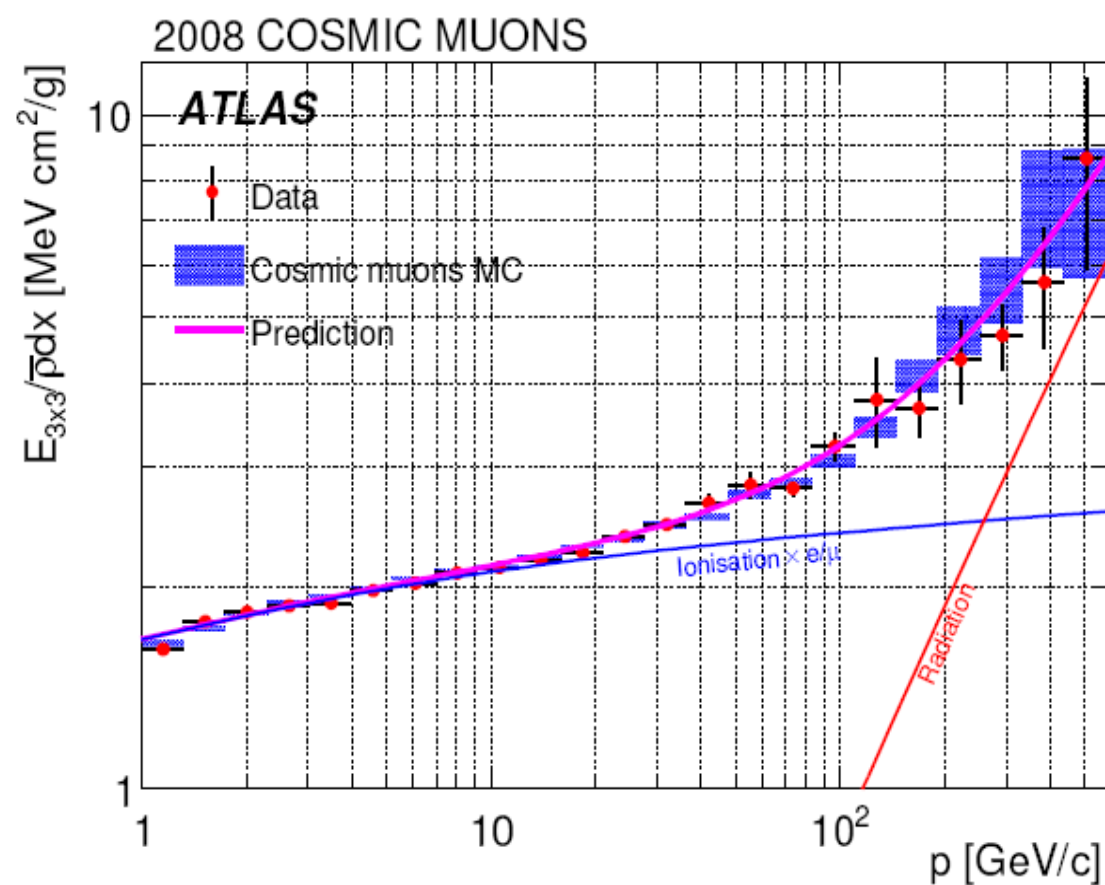


Timing first first beam 2009
better than 1 ns !



dE/dx in the EM Barrel

- Mean energy deposit per unit length as a function of the incoming muon momentum:

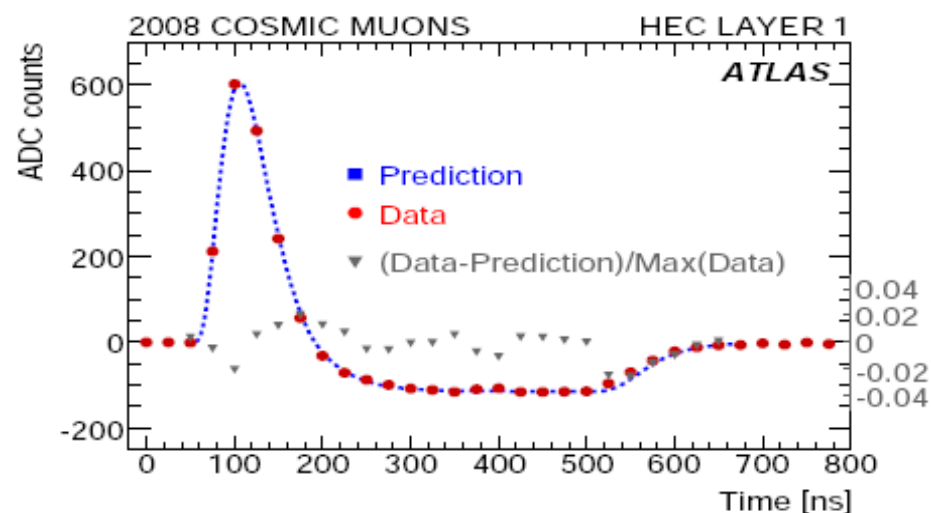
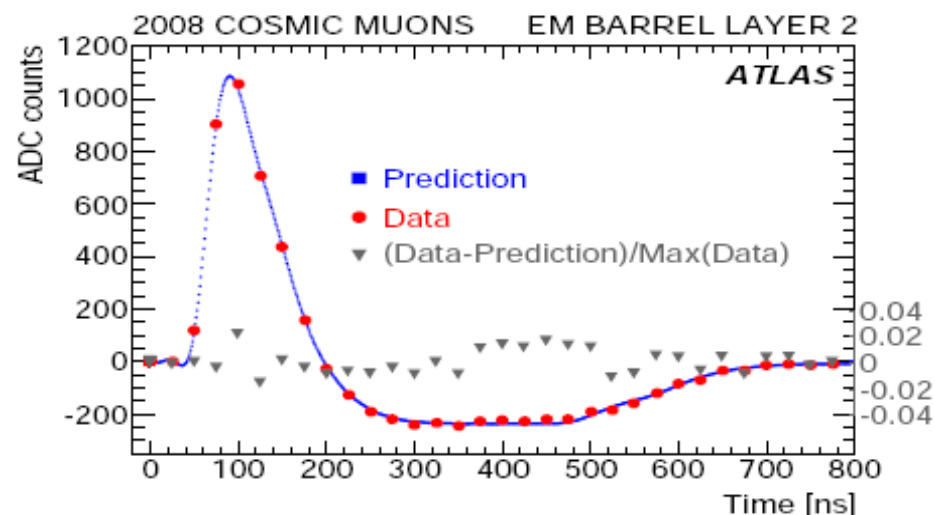


$$\frac{dE}{\rho dx} = \frac{E_{3x3}}{\bar{\rho} L}$$

- E33** = energy measured in a 3x3 clusters (middle layer) taking into account sampling fraction
 - Mean density:** $\rho = 4.01$ g/cm³ from “equivalent” molecule for calo: Pb₃₀ Ar₅₆ Fe₂₄ C₂₁ H₄₁
- Data and MC agree very well
- Also agree with theoretical energy loss from PDG



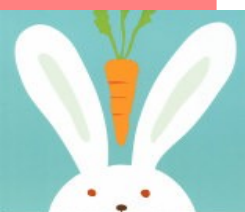
Ionization Pulse Shapes (1/2)



Main ingredient to compute optimal filtering coefficients: need to be precisely known !

- **Prediction** using calibration pulses + cell modeled as resonant RLC circuit
- **Measurement** using 32-sample samples of radiating cosmic muons

→ agreement at the 1-2% level

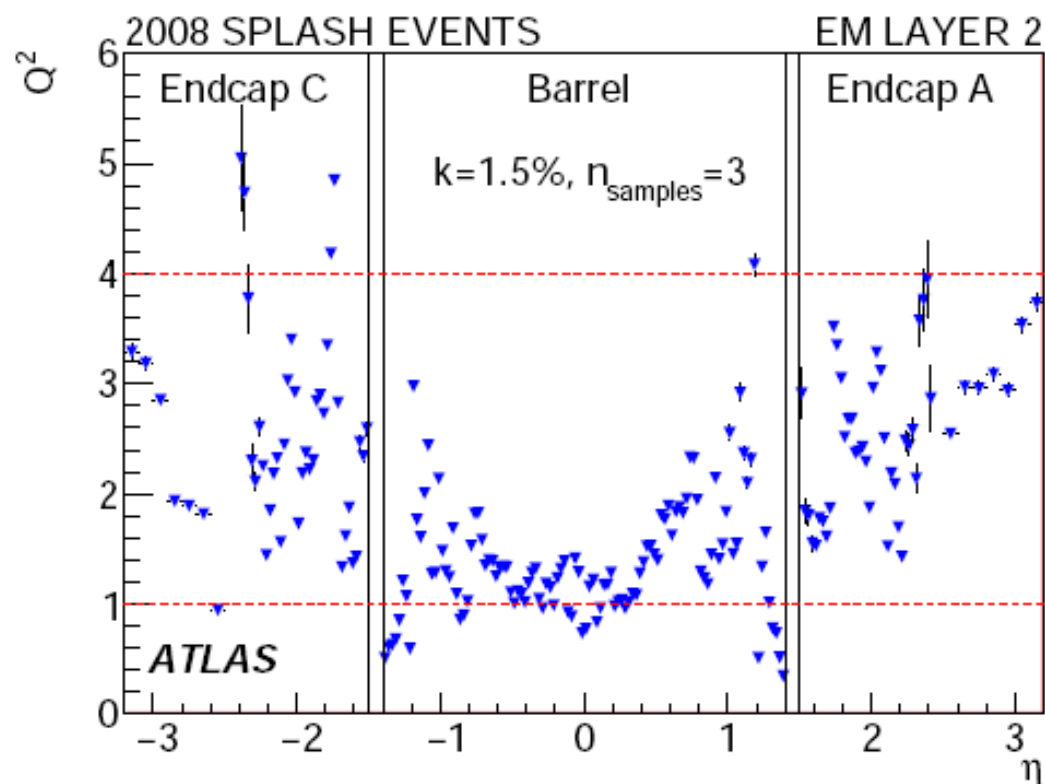


Ionization Pulse Shapes (2/2)

- More quantitative conclusion on signal prediction accuracy obtained by looking at following quality estimator:

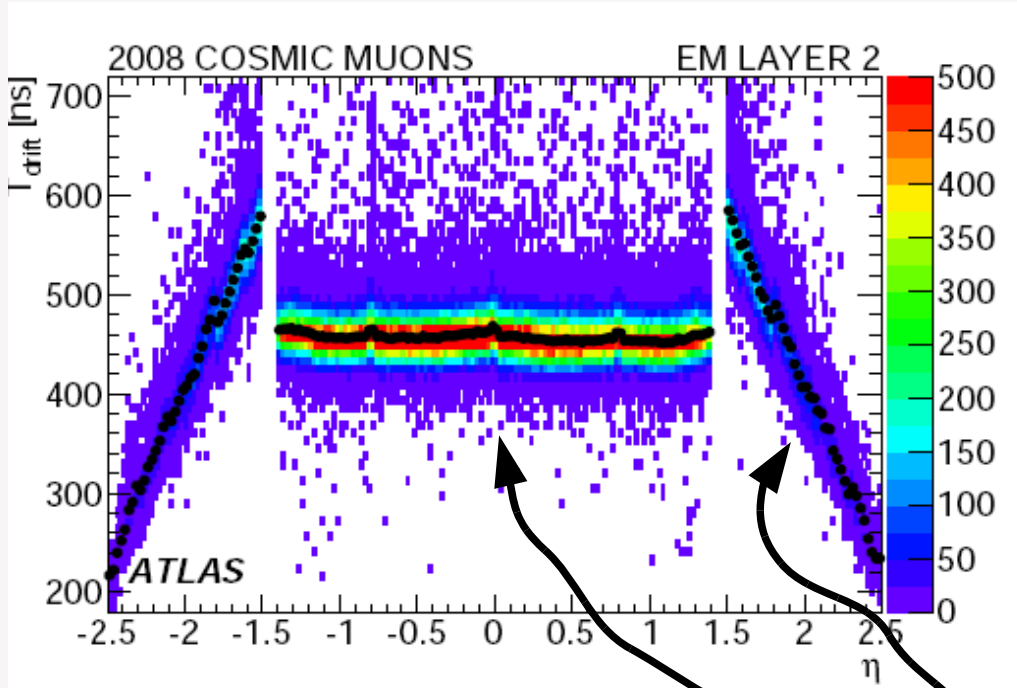
$$Q^2 = \frac{1}{N_{dof}} \sum_{j=1}^{N_{samples}} \frac{(s_j - Ag_j^{phys})^2}{\sigma_{noise}^2 + (kA)^2}$$

- Factor “k” quantifies the relative accuracy on the amplitude:
 - Barrel: $k = 1.4\%$
 - Endcap: $k = 2.6\%$
- Similar to testbeam result where contrib. to constant term due to signal prediction was 0.25%



Ionization Drift Time

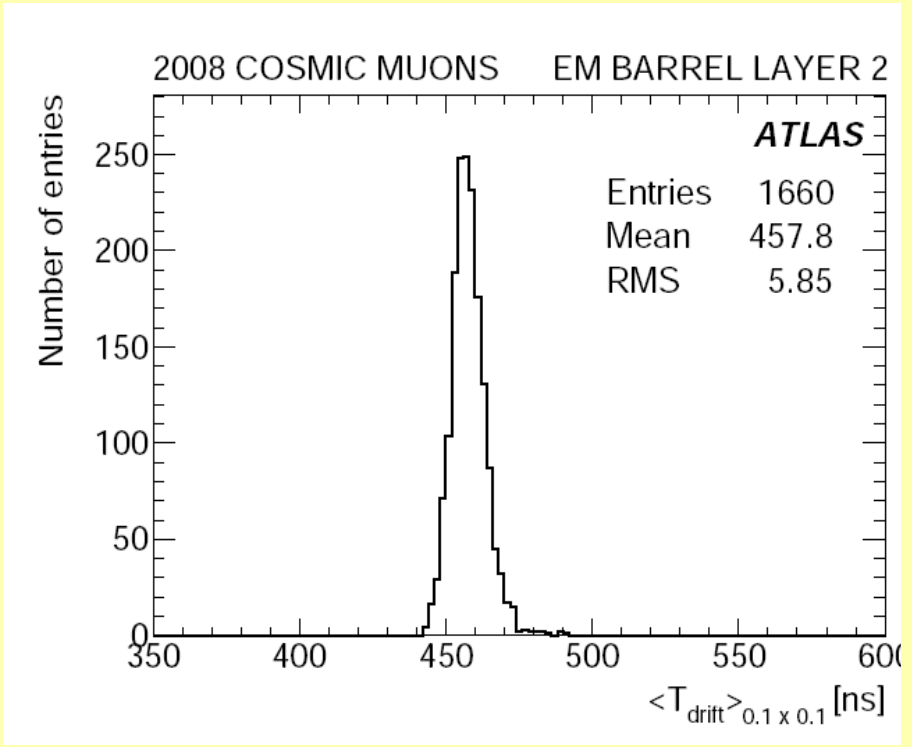
Drift time extracted from fit to the measured pulse
(undershoot region)




$$T_{drift} = \frac{\omega_{gap}^{\alpha+1}}{V^{\alpha}}$$

Constant field in barrel
Varying field in endcap

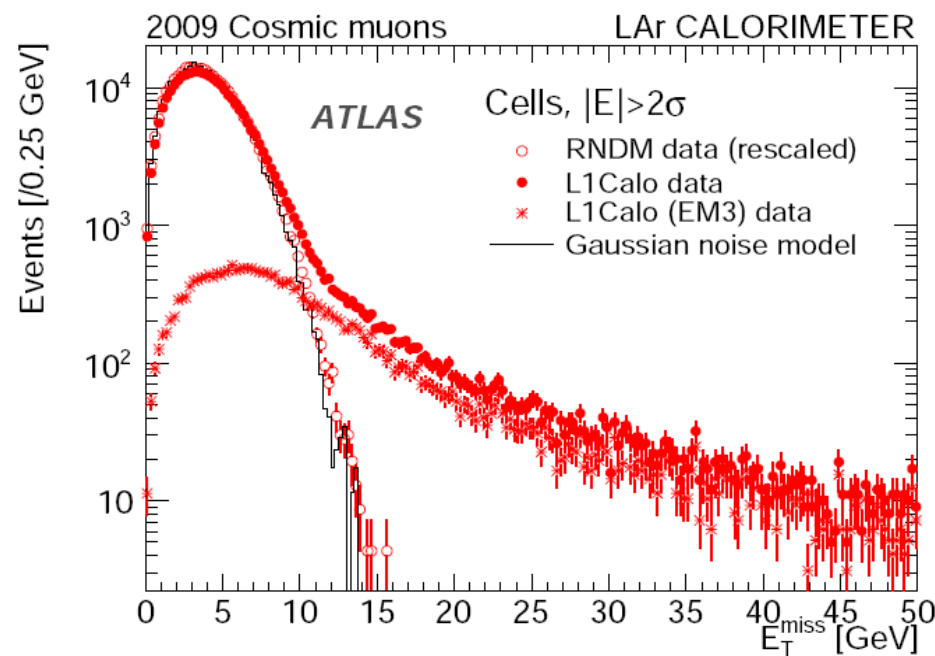
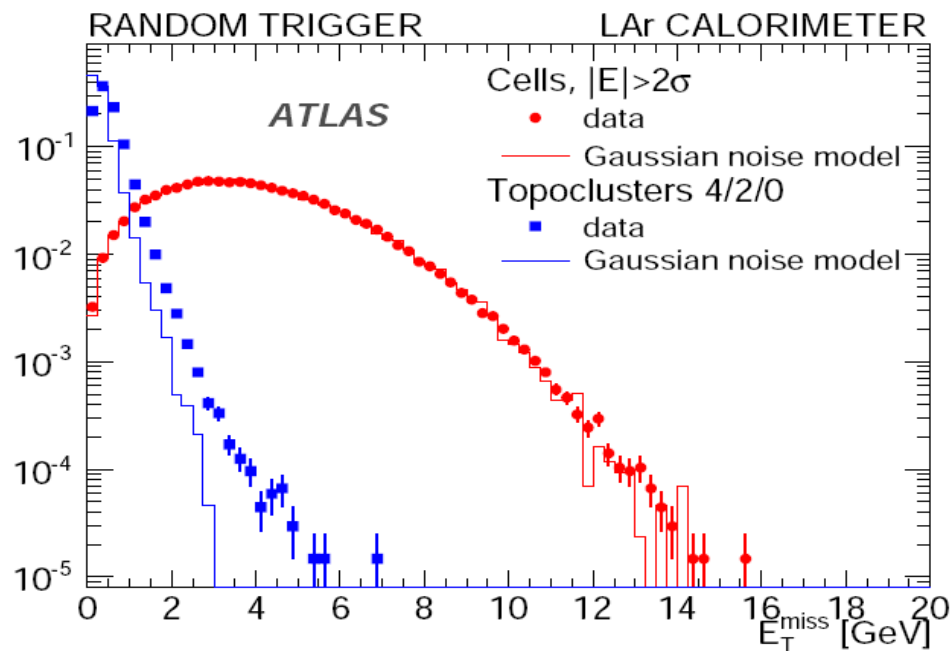
Drift time variations linked to intrinsic calorimeter uniformity:
RMS/mean = 0.29 +- 0.01%
→ upper bound on corresponding constant term
(at construction: 0.16%)



Missing Transverse Energy

- Two noise-suppression methods to compute ET_{miss} :
 - All cells with $|E| > 2 \text{ sigmas_noise}$
 - Topological clusters "4-2-0" 
- Noisy cells are masked
- ET_{miss} measured in random events, and L1Calo triggered events:

		0 σ		
	0 σ	2 σ	0 σ	
0 σ	2 σ	4 σ	2 σ	0 σ
0 σ	0 σ	0 σ	0 σ	



Calorimeter Uniformity: Introduction

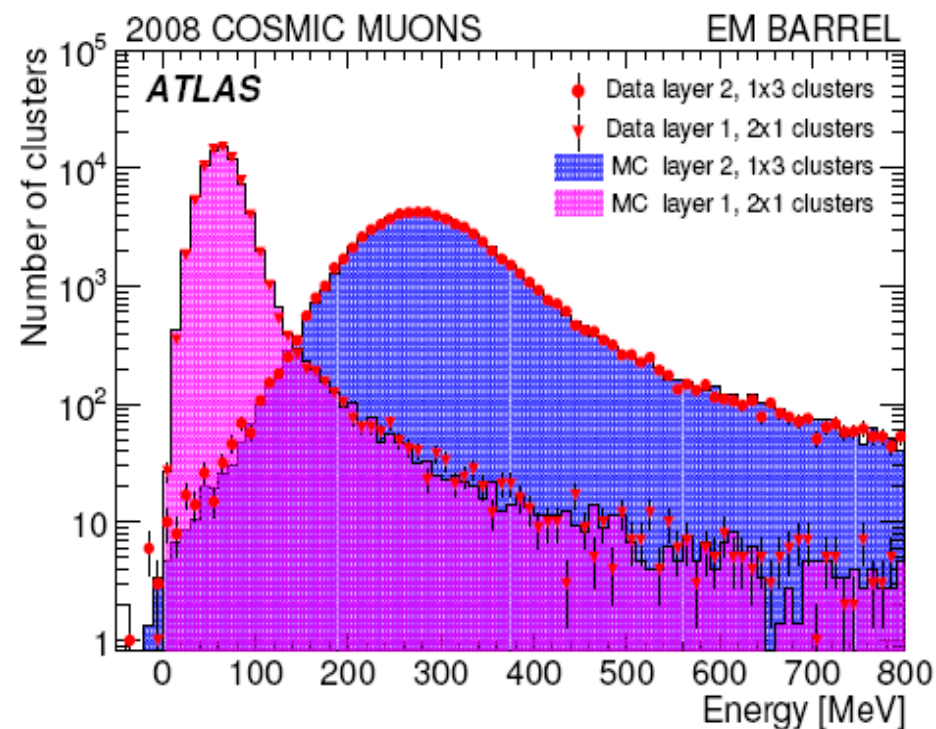
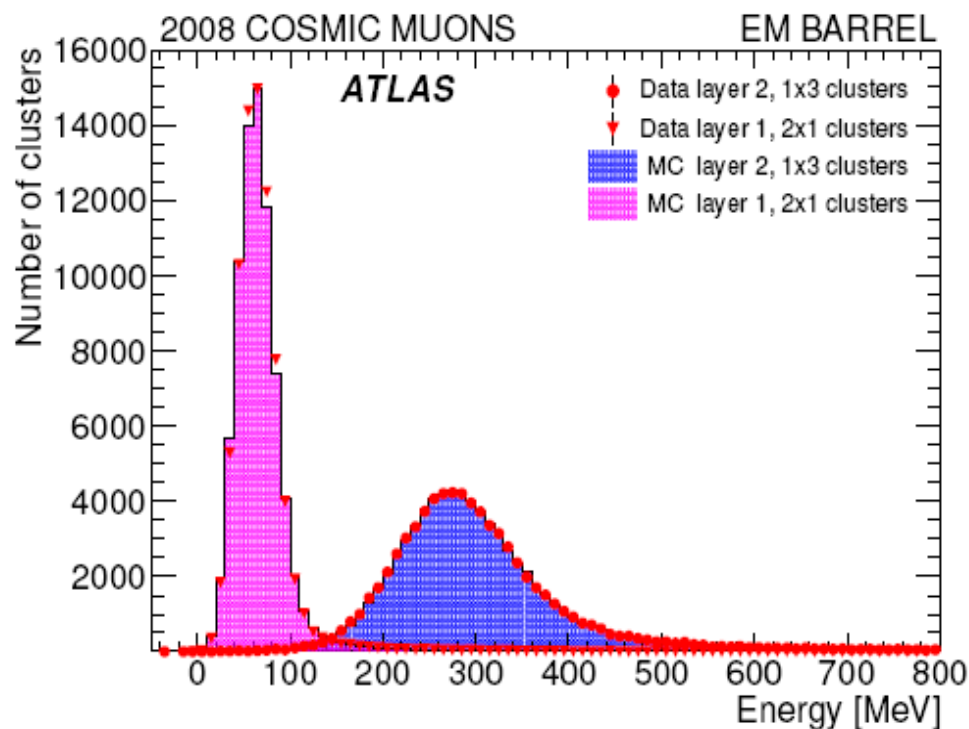


- Cosmic muons used to probe calorimeter uniformity response:
 - Deposited energy proportional to LAr crossed (cell depth)
→ uniformity measured by comparing with MC prediction
 - Muons not sensitive to material as electrons, but allow to measure uniformity cell-by-cell
- Muon energy reconstruction:
 - Use muon **track** to seed calo cluster search
 - Deposited energy in calo reconstructed using **1x3 (middle)** and **2x1 (strips)** clusters
 - **Projectivity/centrality cuts** allow to reduce biases

Calorimeter Uniformity: Energy Lineshapes



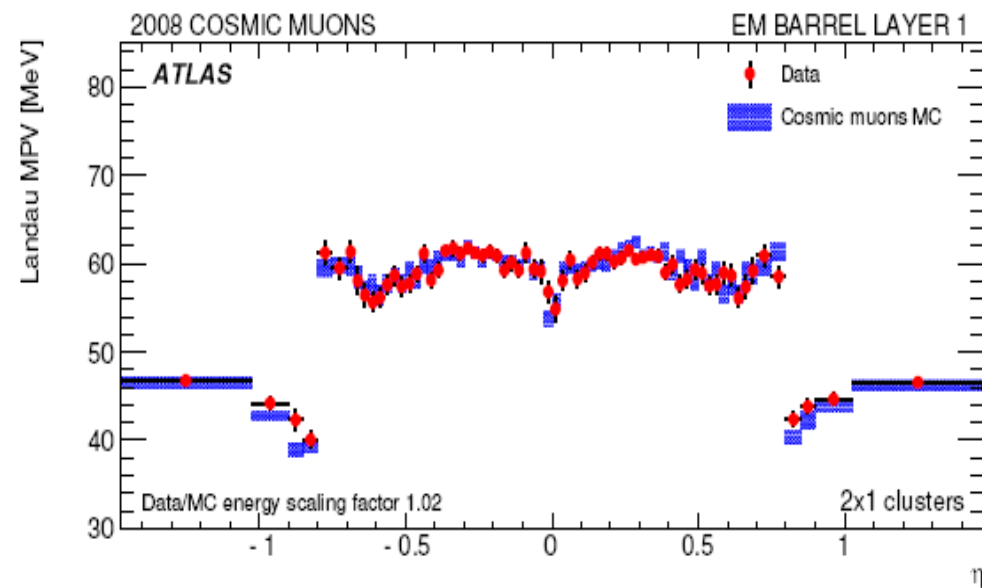
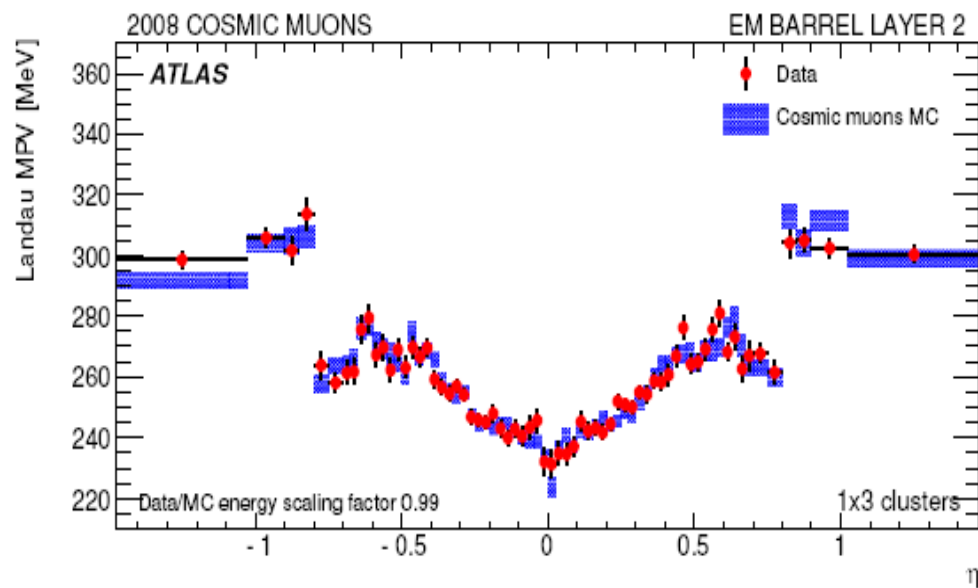
- Agreement between data and MC lineshapes is very good
- **Global energy scale** agrees between MC and data at the **1-2% level**: Impressive !
- Lineshapes are fitted with Landau convoluted with Gaussian:
→ Landau Most Probably Value (MPV) estimates the muon deposited energy



Calorimeter Uniformity: MPVs versus eta



- Limited statistics \rightarrow natural choice to group cells along phi
- Look at Landau MPV along eta for data and MC:
 - Layer 2: typical V-shape due to cell depth variation+ transition at eta=0.8 (lead thickness)
 - Layer 1: flat + transition at eta=0.8



Calorimeter Uniformity

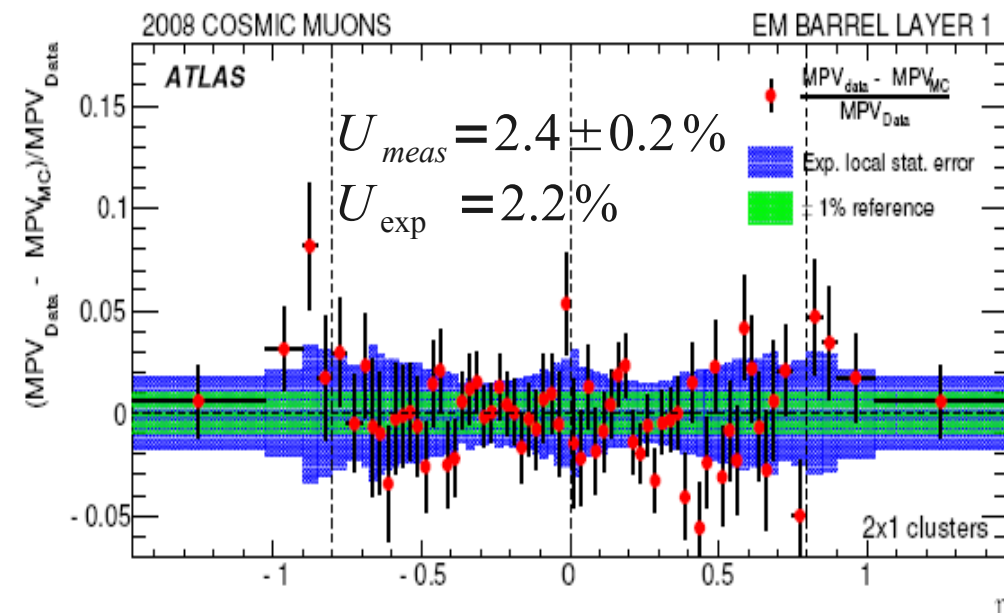
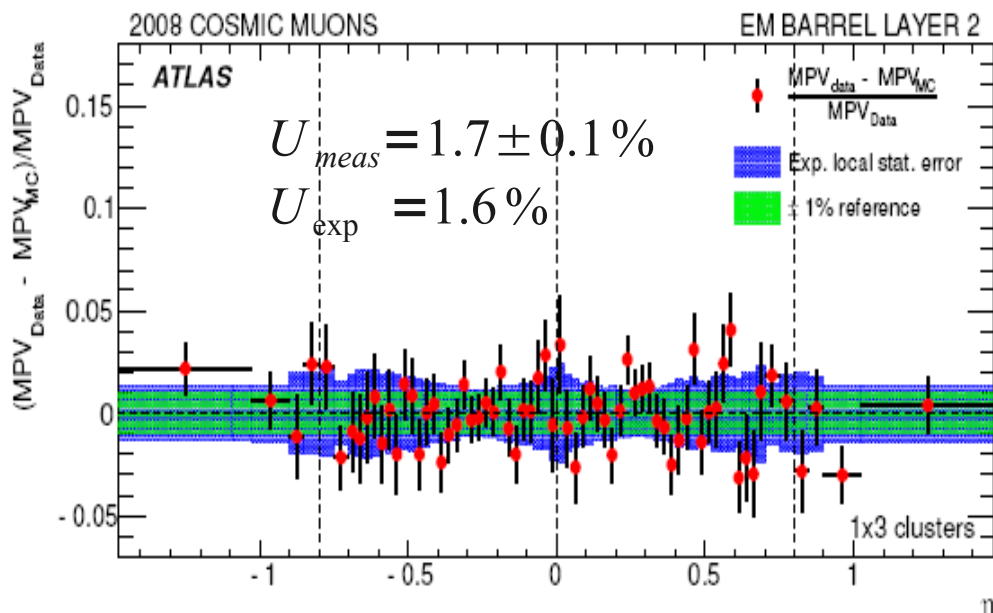


- Measured uniformity (RMS of normalized difference in data and MC MPV):

$$U_{meas} = \sqrt{\sum_{i=1}^{N_{bins}} (U_{i,meas} - \langle U_{i,meas} \rangle)^2 / N_{bins}} \quad \text{with} \quad U_{i,mean} = \frac{MPV_{i,Data} - MPV_{i,MC}}{MPV_{i,Data}}$$

- To be compared with expected uniformity (fluctuations due to noise, ...):

$$U_{exp} = \sqrt{U_{i,Data}^2 + U_{i,MC}^2} \quad \text{with} \quad U_{i,Data(MC)} = \sqrt{\sum_{i=1}^{N_{bins}} \left(\frac{\sigma(MPV_{i,Data(MC)})}{MPV_{i,Data(MC)}} \right)^2}$$



Limits at 95% CL on non-uniformities: 1.1% in middle layer, 1.7% in first layer

Conclusions

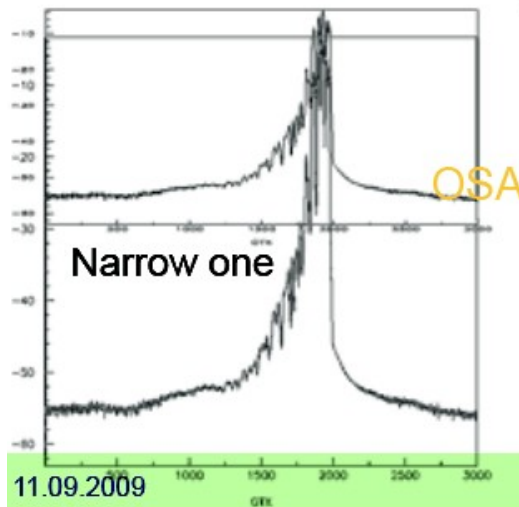
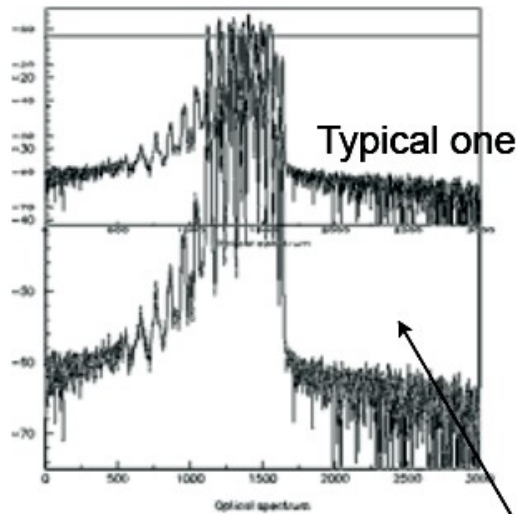
- LAr calorimeter was in very good shape for first collisions:
→ Paolo



Backup

Dying Otx (1/2)

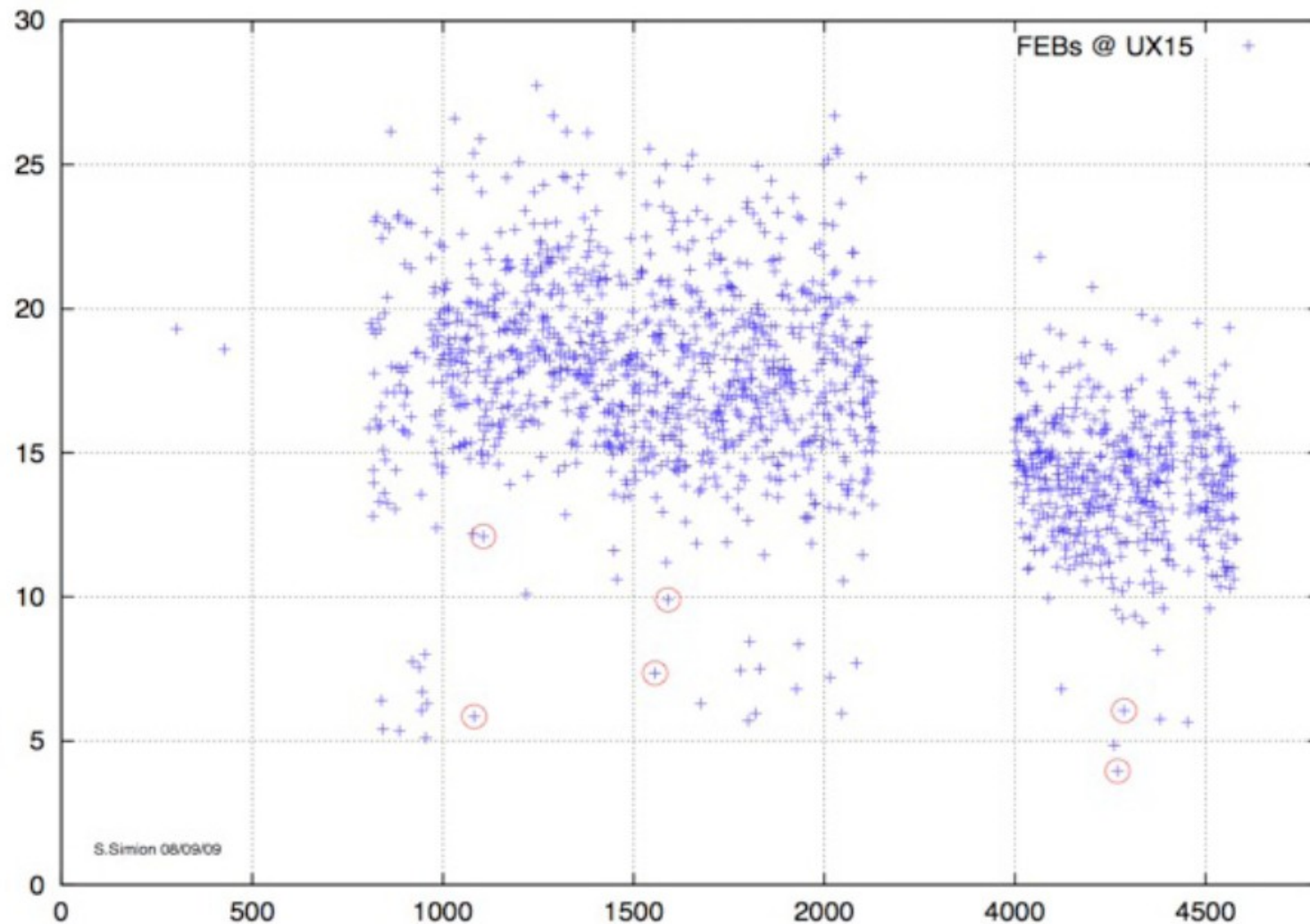
Optical Spectrum: an indicator of End of Life?



OSA

Dying Otx (2/2)

Results: OSwidth vs OTx serial number



○ The six which died after the measurement was performed